The 2nd international conference
on particle physics and astrophysics
ICPPA - 2016
October 10 – 14, 2016, Moscow

TWO-DIMENTIONAL HYBRID SOLID STATE GAS DETECTOR BASED ON ^{10}B LAYER FOR THERMAL AND COLD NEUTRONS

S.Potashev, Yu.Burmistrov, A. Drachev,
S.Karaevsky, E.Konobeevski, S.Zuyev

Institute for Nuclear Research, Russian Academy of Sciences

Application of Slow Neutron Position Sensitive Detector

Slow neutron flux monitor — low reduction of neutron flux is claimed

S.Andriamonje et al. 2D-micromegas detector J. of Korean Phys.Soc.,59(2011)1601-1604

D.S.Ilyin et al, Pos.-sens. thermal neutron monitor. J. of Surface , 9 (2015), 1070-1076.

Small angle scattering(SANS)–high spatial/time resolution&efficiency

P. Strunz et al. SANS-II at SINQ: Riso-SANS facility. Physica B 350 (2004) p.783–786.

V.V.Tarnavich et al. Holmium-yttrium superlattice. J.of Surface, 8(2014)976–982.

V.Lauter-Pasyuk et al. Block-Copolymer Films Appl. Phys. A.19(2003) Suppl.7783-7788.

SANS biomolecule, biocrystal – wavelength near 8A

R.Efremov et al., SANS of lipidic cubic phase behavior in course of bacteriorhodopsin crystallization, J. of Cryst. Grow., 2005, 275, 1453–1459.

SANS Cold neutrons — wavelength more 10A with low reduction

M. Bleuela et al. SANS using VCN Physica B; Condensed Matter 404(2009) 2629–2632.

SANS in Industry – charge/discharge Li-Ion battery in situ

S. Boukhalfa et al. In situ SANS revealing ion absorption in microporous carbon electrical double layer capacitors. ACS Nano, 8 (2014) pp.2495–2503.

New Slow Neutron Pos. Sens.Detector

Helium-3 MWPC- **expensive gas under high pressure leaks and loose properties**

R.Kampmann et al. 2D-MWPC for REFSANS/FRM-II NIM A 529 (2004) pp.342–347

V.A.Andreev..D.S.Ilyin..A.G.Krivshich et al. PSD of TN PNPI PSS 52 (2010)1029-1033.

Solid Boron-10 Detectors – **under low pressure has thin window and low flux reduction. It is suited for cold neutrons**

S Andriamonje et al. Micromegas NIM A 481 (2002) 120–129.

A.I.Drachev, S.I.Potashev. Patent of RF No.2282215, req. 2004-07-01

V.S.Litvin, S.I.Potashev, V.I.Razin, R.A.Sadykov PSWSTCNDetector boron converter.Bull. of RAS. Physics.75(2011)N.2,229-231

G. Gervino et al. NIM A, 718 (2013) pp.143–144.

1.5m cylindrical counter with $^{10}B_4C$ layer of 2.5μm thickness.

M.Kohli et al. NIM A 828 (2016) pp.242–249 (CASCADE).

200x200mm^2 gas chamber with GEM with 6 ^{10}B layers of 1.4μm thickness.

Efficiency = 7.8% for λ=0.6A and 21% for λ=1.82A.

Spatial resolution = 1.4mm. But many electronic channels. Very expensive !

Operating principle

n + ^{10}B→^{4}He (1470 keV) + ^{7}Li (830 keV) + γ (480 кэВ) with a branching ratio 93%;
n + ^{10}B→^{4}He (1730 keV) + ^{7}Li (1310 keV) with a branching ratio 7%.

^{4}He and ^{7}Li are detected in the ion position-sensitive chamber.
Boron surface is not suited as electrode.
Front cathode – 1 mm glass disk with 3 μm layer of ^{10}B, polyimid nanolayer, 0.1 μm aluminium, nanolayer of protective semiconducting polymer.
Rare cathode – 1 mm fiberglass with 63 copper insulated pads of 2 mm width.
Anode – 64 wire plane (wire=W-Re 20 μm). Anode-cathode gap = 2 mm.
Efficiency of detection without aluminum is estimated as 5.5% at λ = 1.8A.

λ =1.82A	λ =4 A	λ =8 A	λ =16 A
5.0%	6.8%	8.8%	10.5%

Multiwire and multipad gas chamber

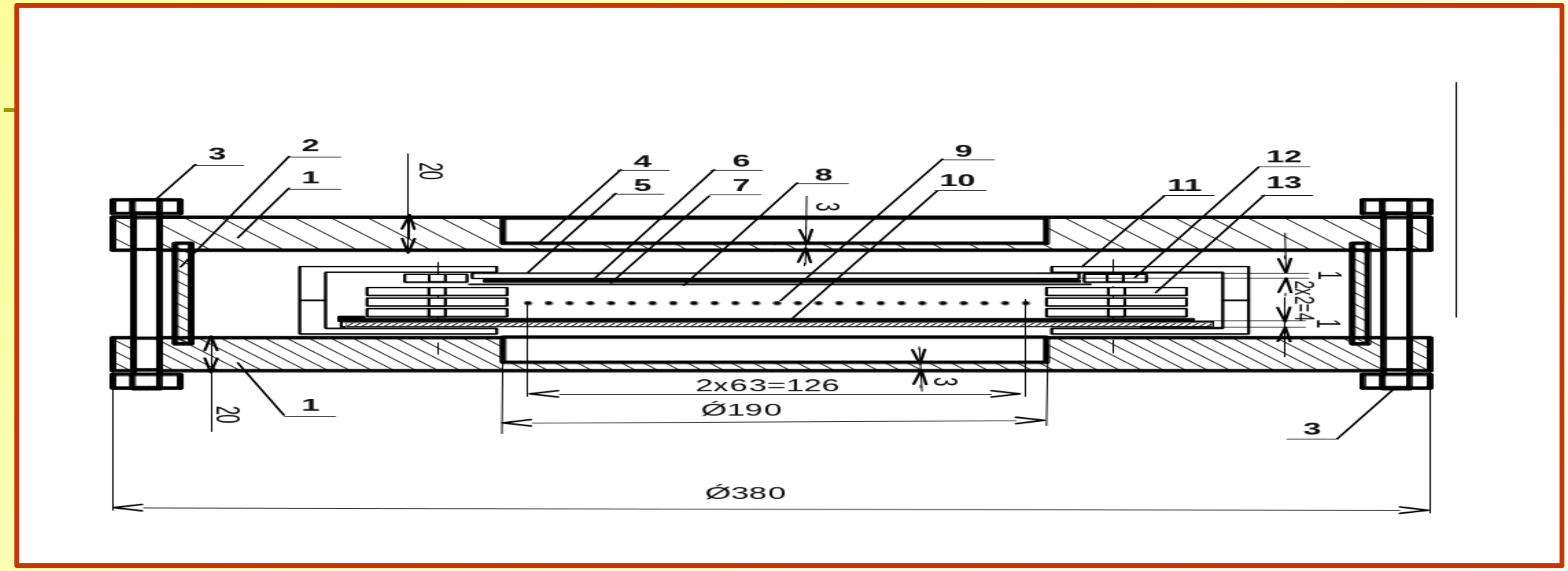

1 — front and rare covers with windows; 2 — cylindrical side wall of housing; 4 — window; 5 — glass disk; 6 — boron-10 layer; 7 — polyimid layer; 8 — aluminum layer; 9 — high voltage and signal wire anode of X coordinate; 10 — signal pad rare cathode of Y coordinate

U= +620V -- +920V. Gas mixture Ar+25%CO_2 + 0.3%CF_3Br. Volume = 3.5 l

A both anode wires and rare cathode pads are connected sequentially to each other through 20Ω resistor

Electronics and Data acquisition system

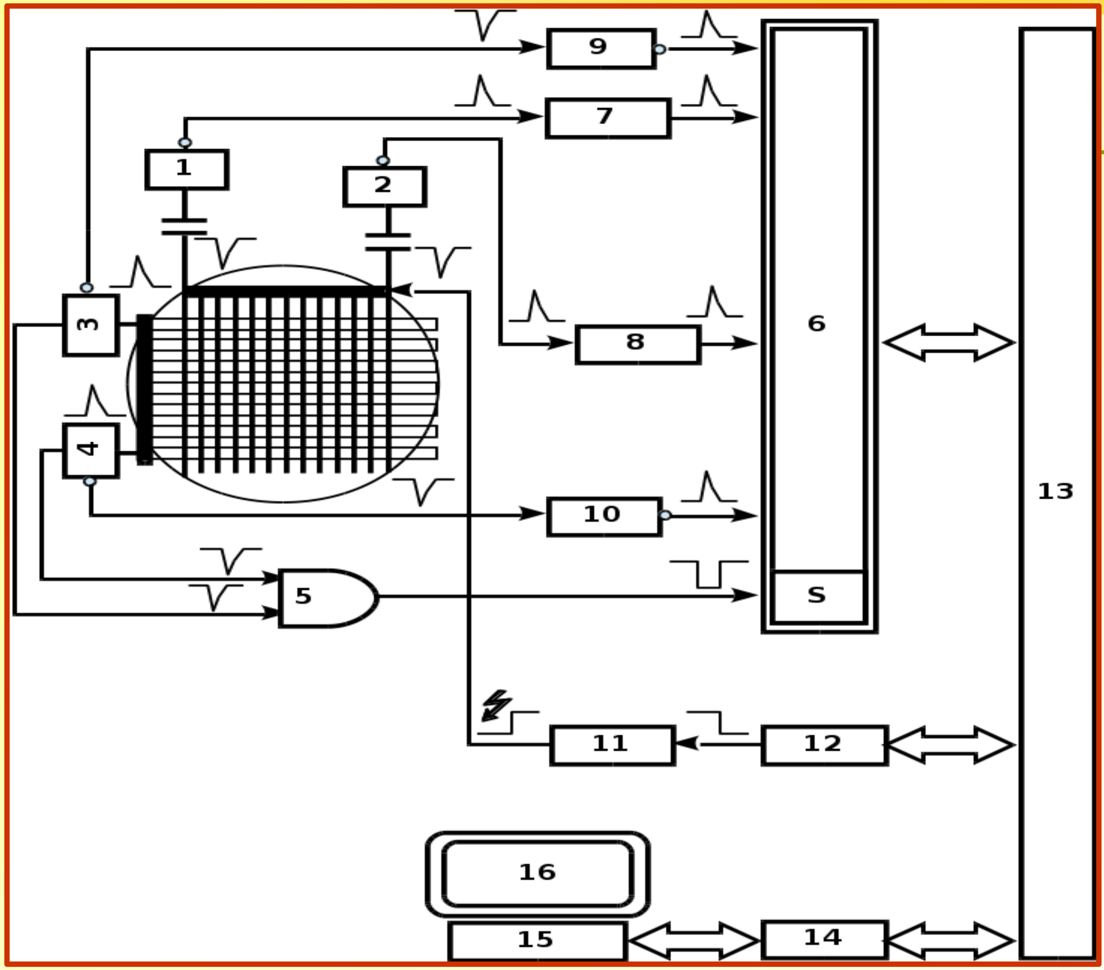

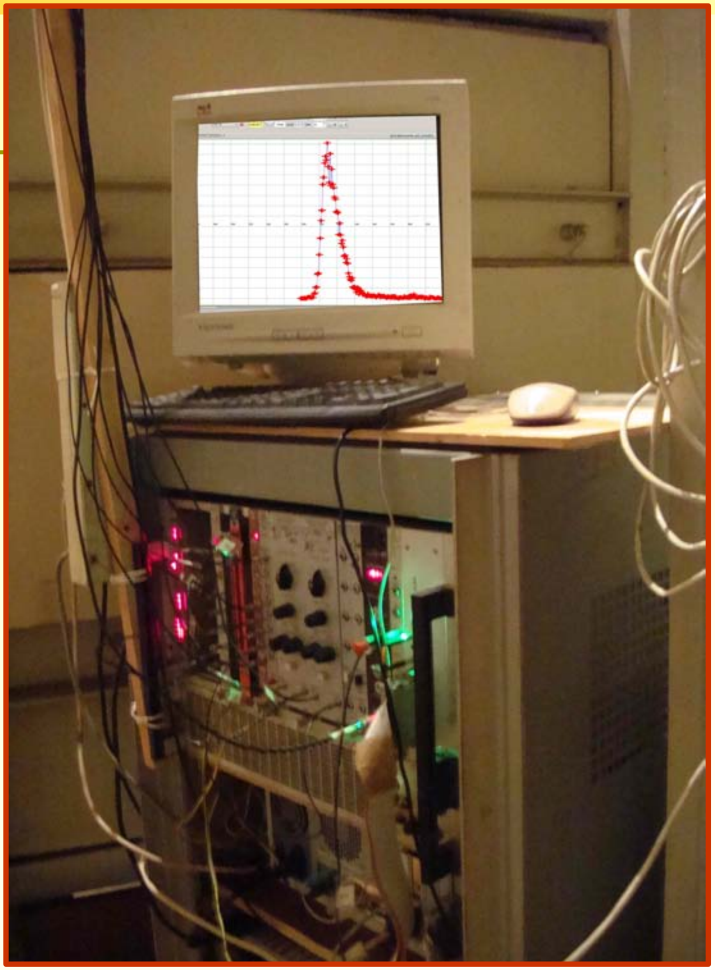

Data acquisition system: **1, 2, 3 and 4 – preamplifiers; 5 - digital discriminator; 6 - amplitude to digital converter; 7, 8, 9 and 10 – amplifiers; 11 - remote control high voltage power supply; 12 – digital to analogous converter; 13 – CAMAC crate bus; 14 – CAMAC crate controller; 15 – PCI branch controller card; 16 – computer.**

Thermal neutron source

Detector is tested using photoneutron source.
Tungsten beryllium photoneutron source (IN-LUE) was created on the base of industrial electron linac LUE-8 operating at electron energy of 7 - 8 MeV with

tungsten electron-gamma convertor,
photoneutron beryllium target and
polyethylene moderator of fast neutrons.

The pulse duration of beam is 3 μs and a bunch frequency is 50Hz.
Maximal flux density of thermal neutrons is evaluated as $\sim 10^7$ cm^{-2} c^{-1}.
Detector is located at a distance of 6 m from the source at an angle of 60^o relative to the electron beam axis

Data analysis: X_1-X_2 correlation at U=700V

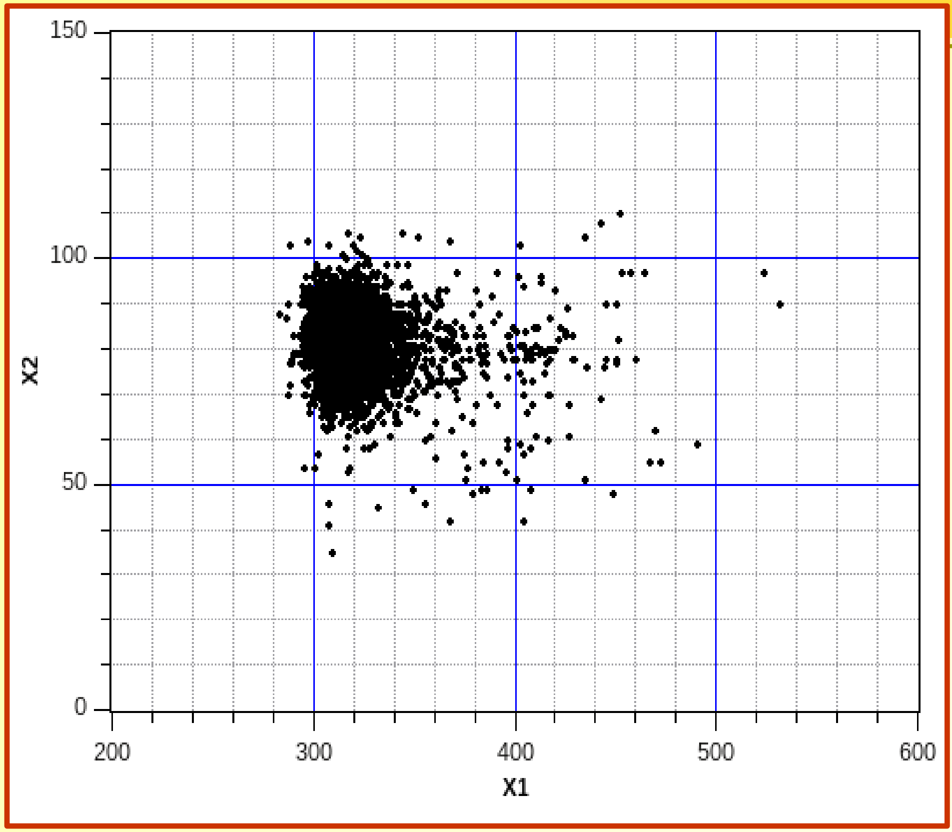

X_1 - X_2 correlation at 700V, 2D-diagram

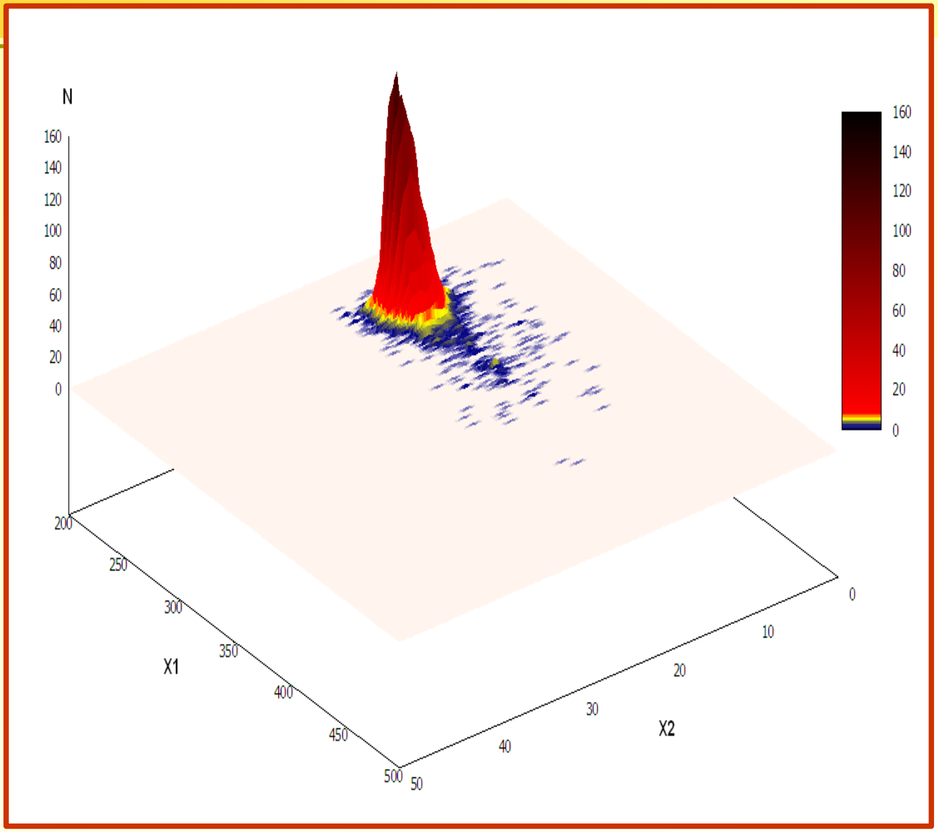

X_1 - X_2 correlation at 700V, 3D-diagram

Counting rate in detector was ~25 c^{-1} at the maximal beam current 40 μA

Pulse height and coordinate spectrum at U=700V

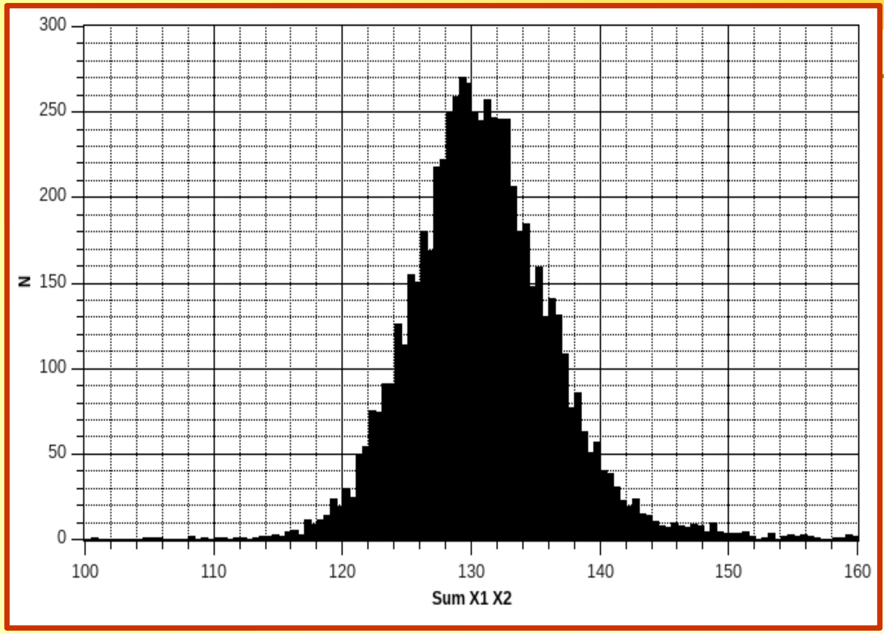

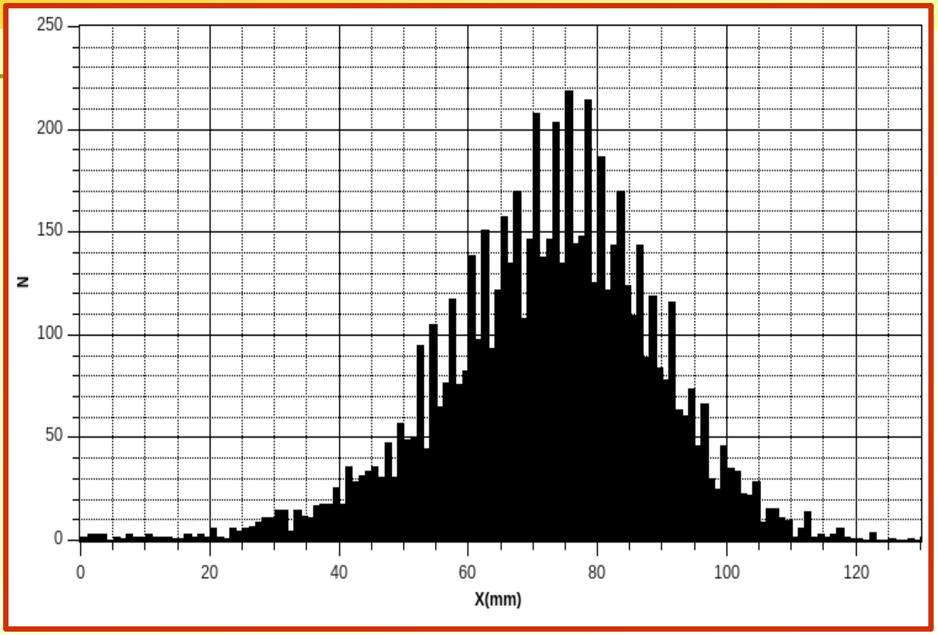

Normalized pulse height spectrum at 700V

X coordinate spectrum at 700V

Pulse height resolution = 15%

$$X = \frac{L(X_{1max} X_2 - X_{2min} X_1)}{(X_{1max} X_{2max} - X_{2min} X_{1min})}$$

Structure in the right spectrum can be explained by a variation of electrical field near and between wires. Structure observed leads to estimate of spatial resolution ~ 2.5mm. Bump shape is related to round shape of glass cathode and non-uniformity of ^{10}B layer.

Data analysis: X1-X2 correlation at U=800V

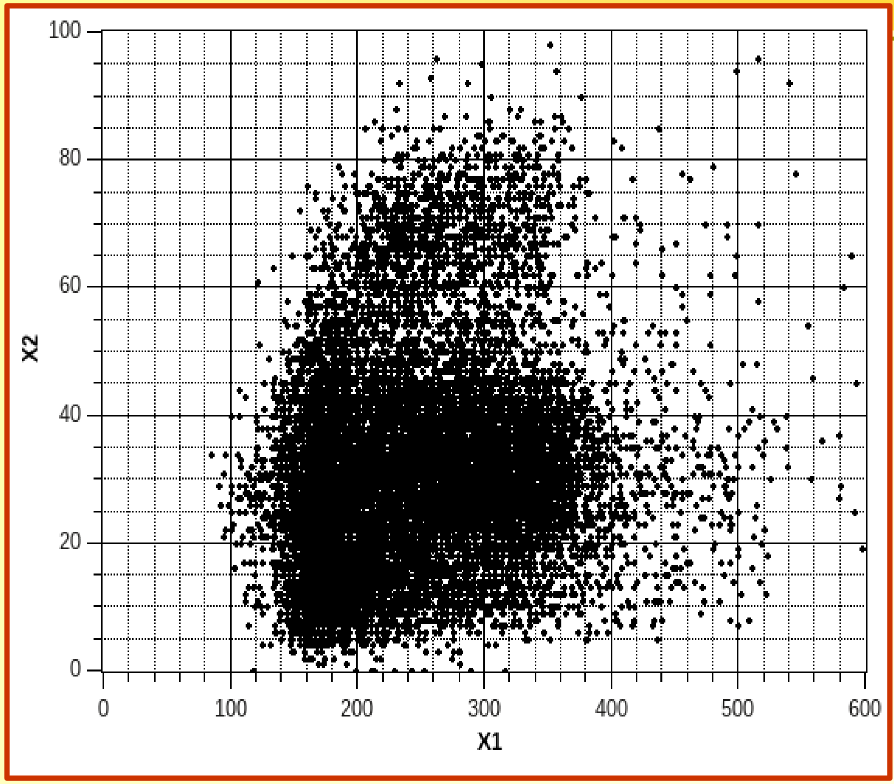

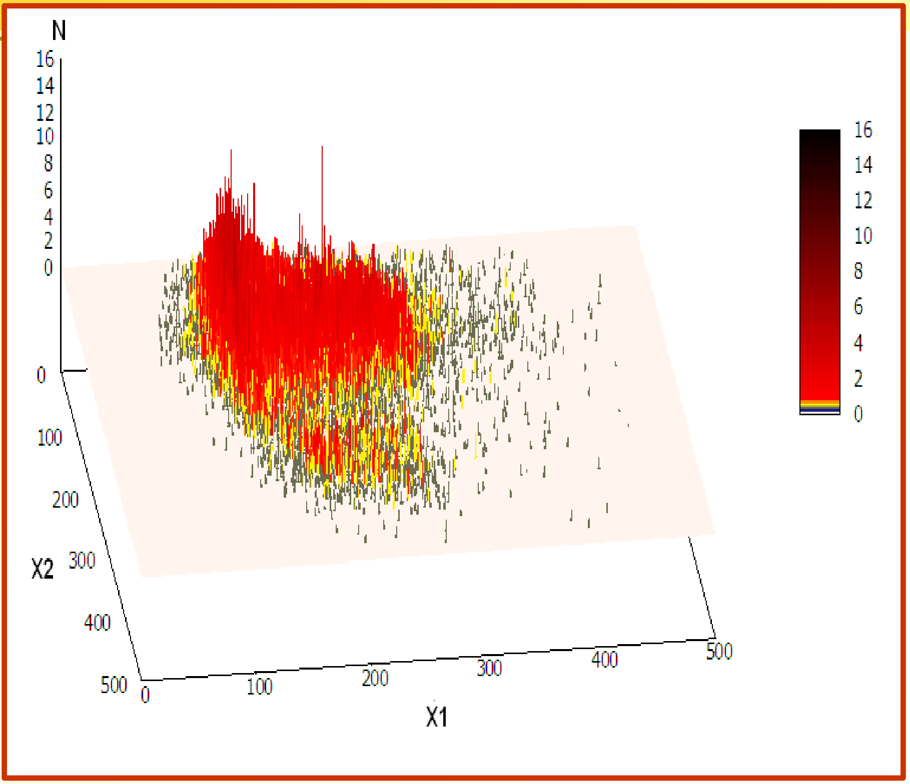

X_1 - X_2 correlation at 800V, 2D-diagram

X_1 - X_2 correlation at 800V, 3D-diagram

Counting rate do not change when voltage increases to 800V. Shape of X_1 - X_2 pulse height correlation becomes wide. Large gas gain leads to fluctuation in an avalanche. Pulse height and, hence, spatial resolution gets worse.

Pulse height and coordinate spectrum at U=800V

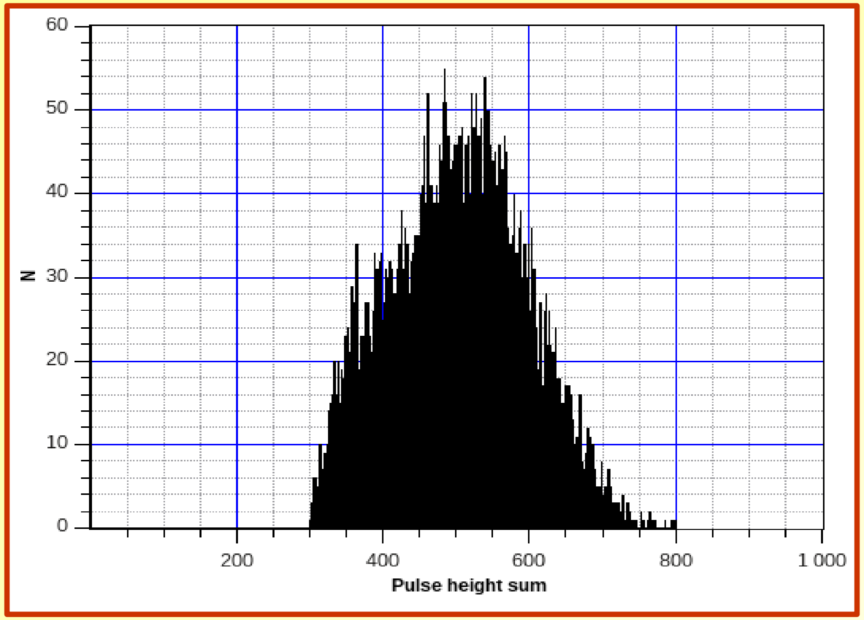

Normalized pulse height spectrum at 800V

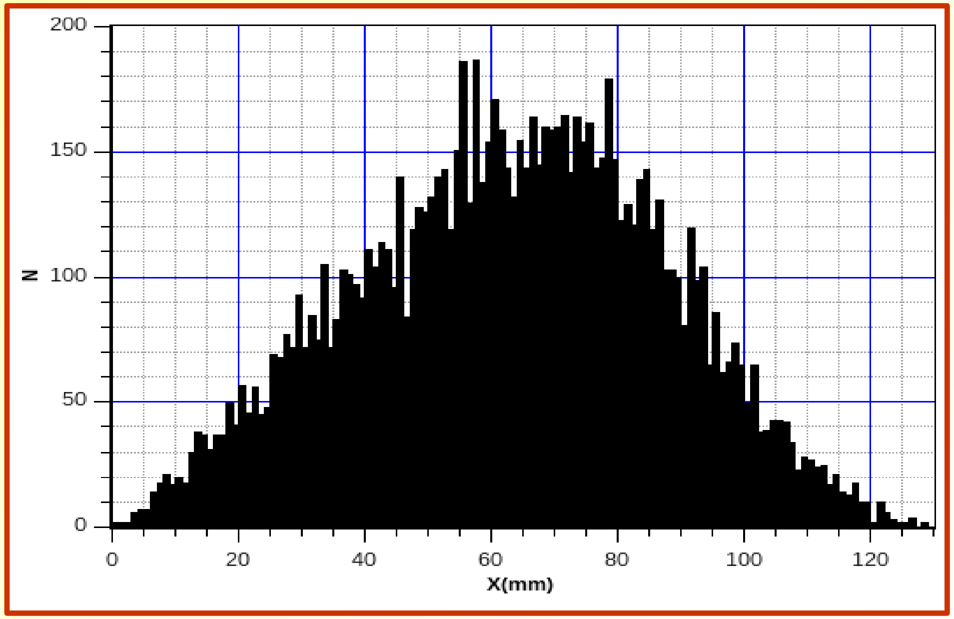

X coordinate spectrum at 800V

Taking into account the geometry of the detector and its disposition and the neutron flux magnitude an estimation of the detector efficiency ~ 4% is obtained. Simulation gives the efficiency from 3% at λ=1.8A and to 6% at λ=8A

X1-X2 correlation at U=650V with diaphragm before detector

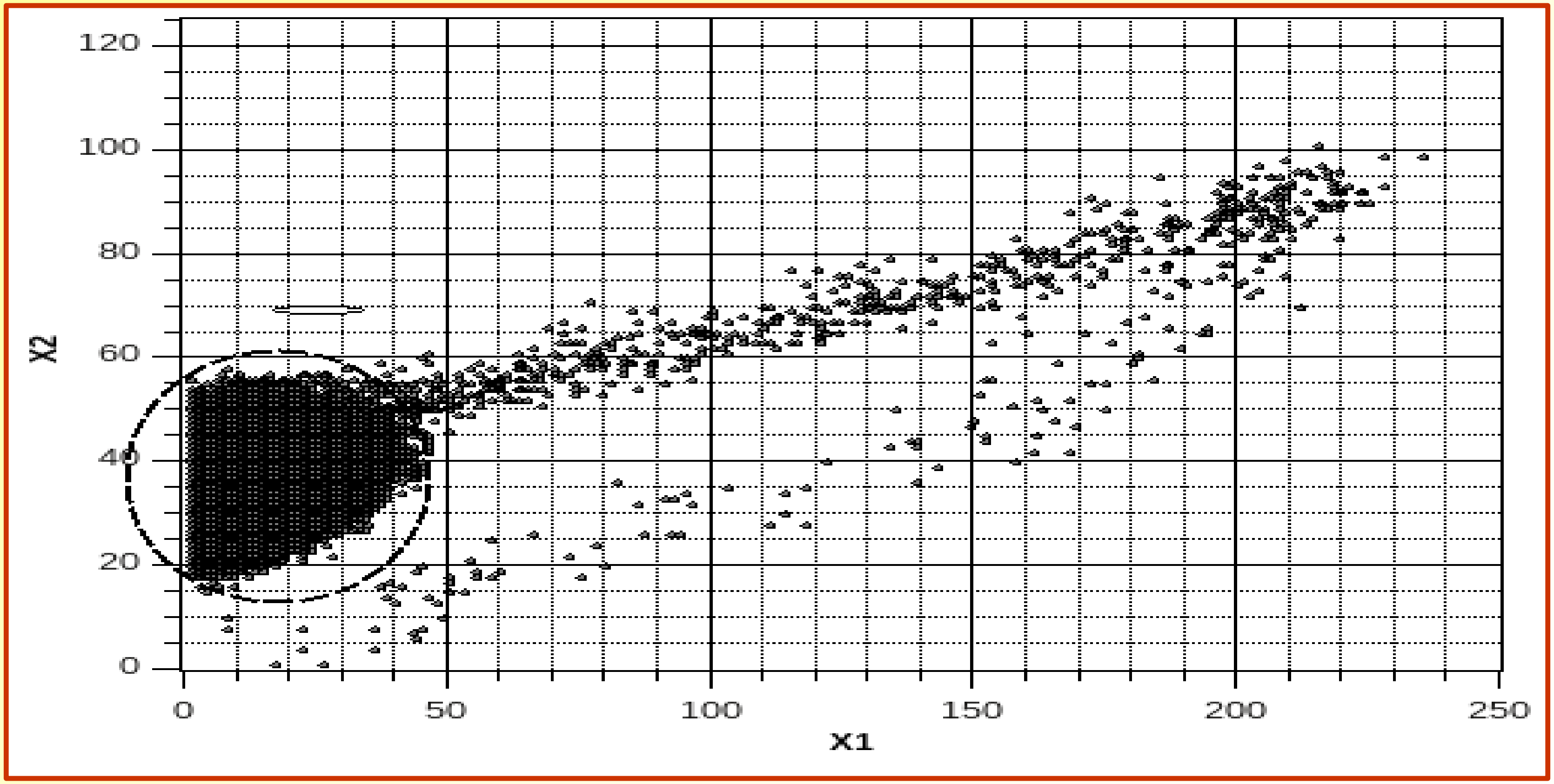

Cadmium diaphragm has 2 mm thickness. Opened part of detector area = 75 mm. Dashed ellipse contains main part of events (99.99%).

Coordinate spectrum with diaphragm at U=650V

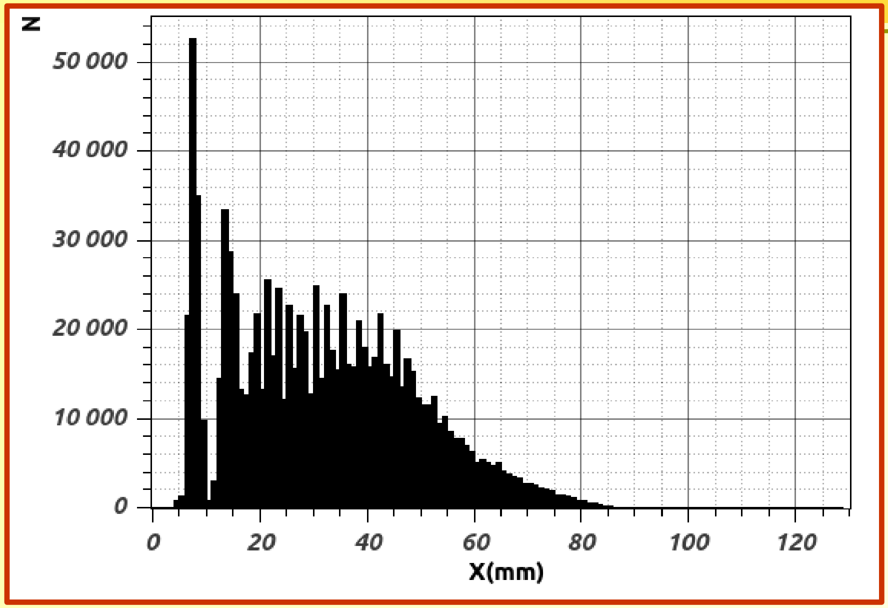

Within the ellipse region, 99.99% events

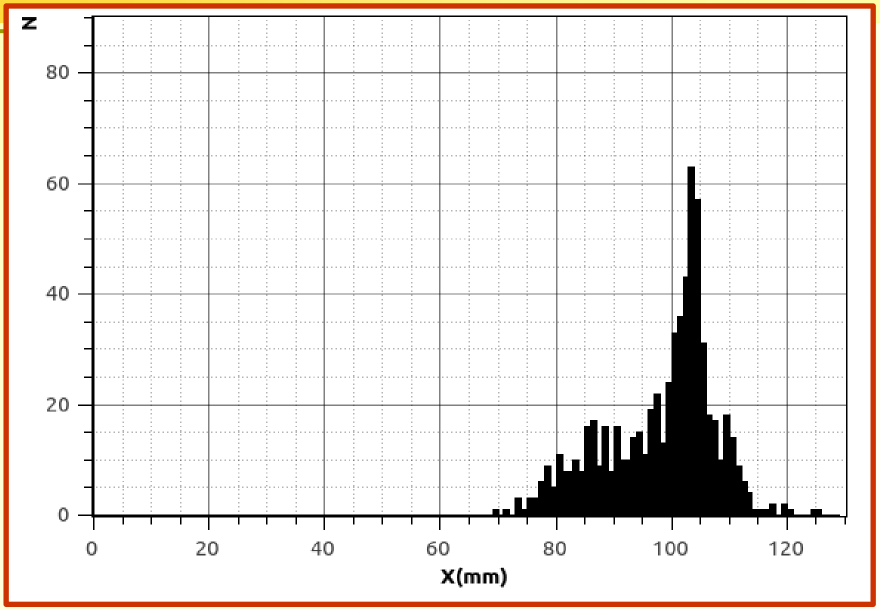

Out of the ellipse region, 0.01% events

Pulse heights for events outside the dashed ellipse are ten times bigger than those for events within the dashed ellipse. They are related to ^{4}He and ^{7}Li nuclei which produce long tracks and move parallel to the anode wire plane.

Counting rate without beryllium target is less than 0.001% of the thermal neutrons one. It corresponds to the background of cosmic thermal neutrons.

Summary and conclusions

- ☎ Position-sensitive slow neutron detector with 3 μm sensitive ^{10}B layer coated by 0.1 μm aluminum layer and gas chamber with active area of 128x128 mm^2 is created and tested. Neutron coordinate is determined by a charge division method.
- ☎ Detector efficiency is estimated from 3% to 6% for thermal neutrons.
- ☎ Ratio of background efficiency to thermal neutron efficiency is less than 0.00001.
- ☎ Pulse height resolution is ~15% and spatial resolution is estimated as 2.5 mm at 700V for the X coordinate for active gas mixture Ar + 25% CO_2 +0.3% CF_3Br in standard conditions.
- ☎ The area uniformity of the detector efficiency is improved with increase of voltage to 800V. However, spatial resolution gets worse.